

1 Article

2 AC iron loss prediction and magnetic properties of 3 Fe–6.5 wt.%Si ribbons prepared by melt-spinning

4 Shuai Wang, Yongfeng Liang *, Biao Chen, Feng Ye and Junpin Lin

5 State Key Laboratory for Advanced Metals and Materials, University of Science and Technology Beijing,
6 Beijing 100083, China; wangshuaizrr@126.com (S. Wang); chenbiaoustb@126.com (B. Chen);
7 yefeng@skl.ustb.edu.cn (F. Ye); linjunpin@ustb.edu.cn (J.P. Lin)

8 * Correspondence: liangyf@skl.ustb.edu.cn; Tel.: +86 10 82376643

9 **Abstract:** Ultra-thin Fe–6.5wt.%Si ribbons with 35 μm in thickness were prepared by
10 melt-spinning. The magnetic properties were investigated before and after annealing 1000 °C. DC
11 properties and low-frequency (400 Hz ~ 10 kHz) iron losses have significantly improved after heat
12 treatment. A simplified formula based on Steinmetz law which can be used to predict the AC iron
13 loss is presented. According to the results of some iron losses data, a simplified formula has been
14 determined, and the extent of AC iron losses can be predicted. The results obtained from the
15 formula predict AC iron loss to a good degree. The method developed in this work could be
16 extended to other magnetic materials for predicting AC iron loss with greater ease.

17 **Keywords:** Fe–6.5 wt.% Si; Ribbon; Melt spinning; AC iron loss prediction; Magnetic properties

18

19 1. Introduction

20 Silicon steels are mainly used in transformers, power generators and motors as important soft
21 magnetic materials. In these, core loss occurs due to hysteresis and eddy current circulation during
22 usage, wherein the hysteresis loss is linear to frequency, and the eddy current loss is proportional to
23 the square of the frequency. Therefore, eddy current loss accounts for a large proportion in high
24 frequency use.

25 Compared with the ordinary silicon steel, Fe-6.5wt.%Si (high silicon steel) alloy has many
26 advantages in magnetic properties, such as its properties of near zero magnetostriction, high
27 permeability, high resistivity, low noise and low core loss[1]. The high resistivity aids in the
28 suppression eddy current and thus leads to a significant reduction in eddy current loss.

29 However, due to the brittleness of Fe-6.5wt.%Si originated from ordered phases of B2 and D0₃
30 [2,3], it is extremely difficult to produce the Fe-6.5wt.%Si alloy by traditional hot-cold rolling process.
31 Rapid solidification can suppress the transformation of ordered phases due to great cooling rate, and
32 thereby enhance the ductility [4]. Melt-spinning can be used for refining grains [5] and preparing
33 magnetic material ribbons with good magnetic properties [6]. Previously, high-silicon steel ribbons
34 of 25 mm width were prepared by melt-spinning [7]. In this paper, various heat treatments were
35 applied to the as-spun Fe–6.5 wt.% Si ribbons. The relationship between microstructures and
36 magnetic properties was investigated. In addition, a method based on Steinmetz law for prediction
37 of iron loss is presented and verified.

38 2. Materials and Methods

39 Herein, Fe–6.5wt.%Si ribbons with 35 μm thickness were used. The composition of the ribbons
40 measured by chemical analysis was Fe: 93.54 wt.%, Si: 6.46 wt.%. Micromorphology and
41 cross-sections of the ribbons were observed using the SEM.

42 For magnetic properties measurement, the Fe–6.5wt.%Si ribbons were cut into 10 mm wide and
43 subsequently coated with MgO powders which plays the dual roles of insulation and adhesion
44 prevention. Moreover, the ribbons were wound into a toroidal core of 32 mm inner and 40 mm inner
45 and outer diameter respectively (Figure 1 inset). The alternating current (AC) and direct current

46 (DC) magnetic properties were measured using the NIM-2000S AC and NIM-3000S DC instruments
 47 respectively. B_8 , B_{50} were tested at magnetic field strength of 800 A/m, 5000 A/m respectively.

48 To explore the changes in magnetic properties with greater accuracy and reduce the number of
 49 errors caused by differences between the different samples, the same core was tested over five
 50 rounds of measurement. It should be noted that first the core was tested without heat treatment and
 51 subsequently it was annealed in an Ar atmosphere at 1000 °C for 0.5 hour (referred to as 0.5 h),
 52 following which the magnetic properties were tested. Subsequently, the same core was heated in an
 53 Ar atmosphere at 1000 °C for plus 1 hour (referred to as 1.5 h), then 1000 °C for plus 1.5 hours
 54 (referred to as 3 h) and then plus 2 hours (referred to as 5 h). After each heat treatment, magnetic
 55 properties were tested, as well as the grain sizes to be observed.

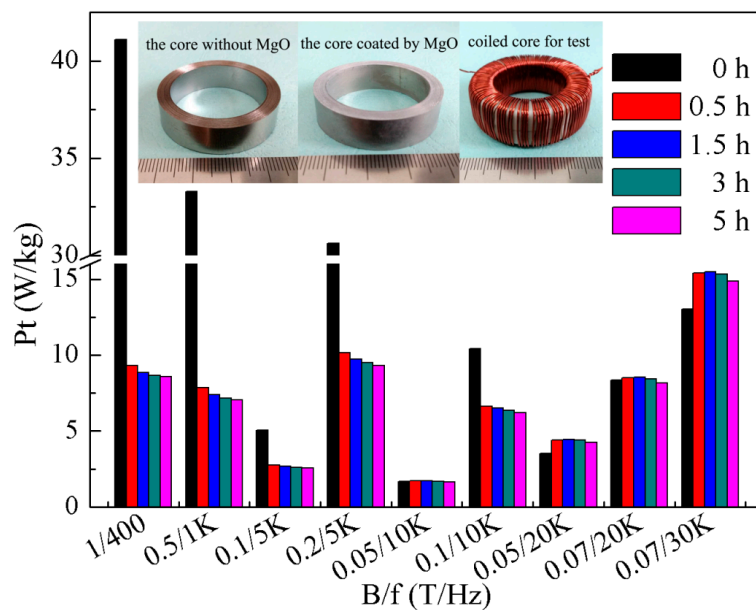
56 3. Results and Discussion

57 The DC properties of Fe-6.5wt.%Si ribbons are shown in Table 1, and it is evident that the DC
 58 properties has been greatly improved after the 1000 °C heat treatment, which is reflected in the
 59 improvement of the magnetic permeability, B_8 and reduction in coercivity value.. It is observed that
 60 there is almost no change in B_{50} before and after heat treatment, owing to the sufficiently large
 61 magnitude of the external magnetic field, resulting in the same value of the magnetic induction due
 62 to an identical arrangement of the magnetic domain.

63 **Table 1.** DC properties of Fe-6.5wt.%Si ribbons.

sample	μ_m	B (T)		Hc (A/m)
		B8	B50	
0 h	1,843	1.16	1.55	237.6
0.5 h	10,589	1.31	1.55	48.9
1.5 h	10,931	1.31	1.55	46.6
3 h	11,082	1.31	1.55	45.7
5 h	11,051	1.32	1.56	45.3

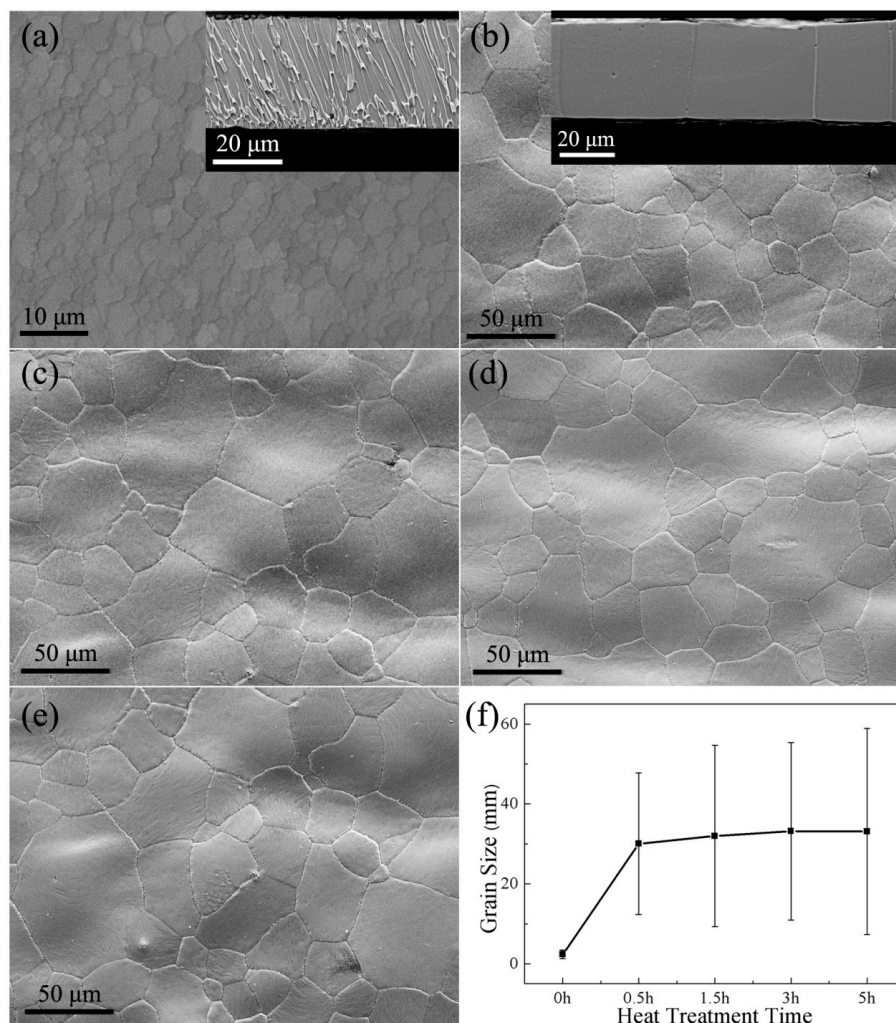
64
 65 Figure 1 presents the values of AC iron losses. The iron loss corresponding to the frequency
 66 range between 400 Hz and 10 kHz shows a decreasing trend with heat treatment at 1000 °C. For
 67 frequencies higher than 10 kHz, the iron loss increases compared to the as-spun state. Figure 2 (a) ~
 68 (e) show the free surfaces of the ribbons and Figure 2 (f) depicts the grain sizes on the free surface
 69 with respect to the annealing time. Figure 2 (a) and (b) insets represent the longitudinal sections of
 70 the ribbons before and after heat treatment. The original ribbons consist of equiaxed grains on the
 71 wheel surface (the surface contacting the copper roller) and columnar grains on the free surface (the
 72 surface not contacting the roller). The grain size is small and uniform. After subjecting to 1000 °C
 73 for 0.5 hour, each grain extends through the entire thickness, and the grain size increases from a few
 74 microns to about 30 microns. With increasing the heat treatment time, the grain size tends to
 75 increase but very slowly. The ribbon surfaces would hinder the growth of grain size [8]. After heat
 76 treatment, the grain growth results in reduction of grain boundaries, which aids in the reduction of
 77 the obstacles of the movement of magnetic domains, thereby reducing the hysteresis loss.
 78



79

80 **Figure 1.** Iron losses corresponding to different conditions before after heat treatment; the inset represent the
 81 samples for test.

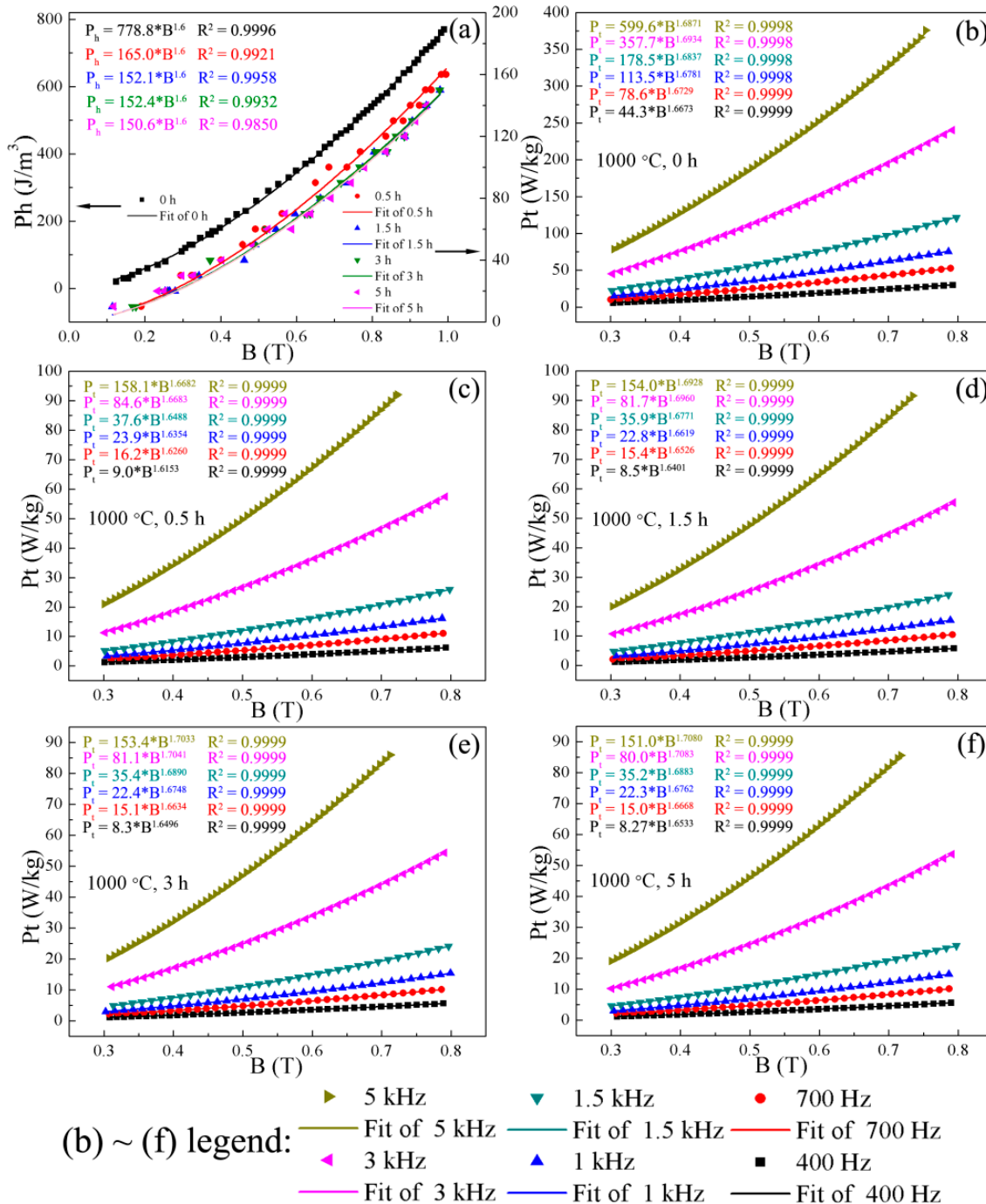
82



83

84 **Figure 2.** Free surface microstructure of Fe-6.5wt.%Si ribbons (a) in absence of heat treatment; (b) of 1000 $^{\circ}\text{C}$, 0.5
 85 h; (c) 1000 $^{\circ}\text{C}$, 1.5 h; (d) 1000 $^{\circ}\text{C}$, 3 h; (e) 1000 $^{\circ}\text{C}$, 5 h. (f) Grain size statistics.

86 Figure 3 depicts the results of the hysteresis loss curves and the AC iron loss curves. It is well
 87 known that the Steinmetz law [9] is used to describe the relationship between P_{hys} (hysteresis loss)
 88 and B_m (maximum magnetic induction), wherein: $P_{\text{hys}} = k_h B_m^n$ at DC field, where, k_h is the
 89 hysteresis loss coefficient, and n is the exponent of B_m , which is always near 1.6. The different color
 90 formulas in the Figure 3 (a) represent the fitting results of DC iron loss for different heat treatment
 91 time. R^2 is the goodness of fit and the closer the value is to 1, the better the fit is. From Figure 3 (a),
 92 the DC iron losses decrease drastically after heat treatment and trends to decrease with extension of
 93 duration of heat treatment and the coefficients of the fitted results (“ k_h ” values) also have such a
 94 tendency. Generally, the “ k_h ” value is affected by the kind of material, thickness, stress, grain size,
 95 etc. Any factor that reduces the resistance of magnetic domain motion can reduce the “ k_h ” value.
 96

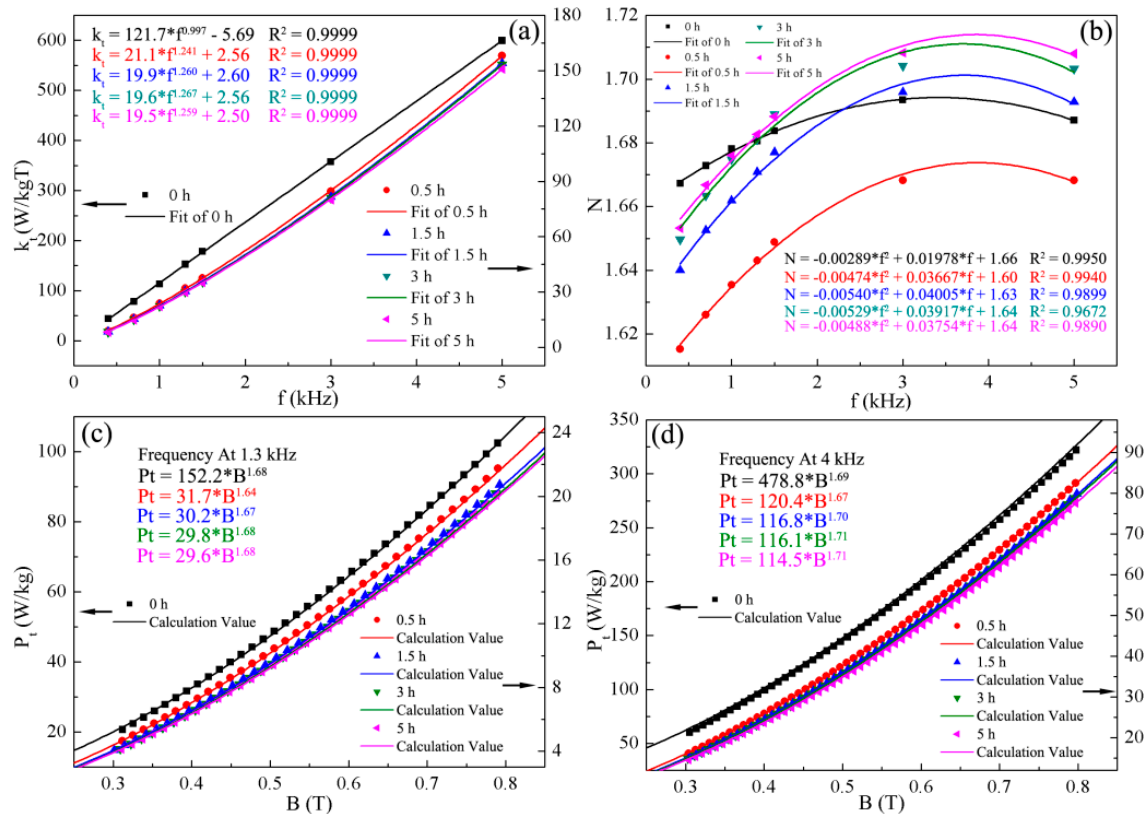


97
 98
 99
 100

Figure 3. AC and DC iron losses and fit results before and after heat treatment, (a) DC iron losses - magnetic induction curves; (b) ~ (f) AC iron losses - magnetic induction curves at different frequencies. R^2 is the goodness of fit wherein, the closer the value is to 1, the better the fit is.

101 Ever since Steinmetz formulated the law, many modifications have been proposed, such as the
 102 “AC Steinmetz law”: $P_t = k_{ac} B_m^n f^\alpha$, where f is the AC frequency [10,11]. And upon comparing
 103 hysteresis loss curve and AC iron loss curve from Figure 3, it can be seen that their shapes are
 104 similar, exhibiting as monotonically increasing concave functions. Here, we simplify the AC
 105 Steinmetz law into $P_t = k_t B_m^N$ similar to “Steinmetz law” $P_{hys} = k_h B_m^n$ and different to “AC
 106 Steinmetz law” $P_t = k_{ac} B_m^n f^\alpha$ wherein “ k_h ” is defined as a function of microstructure and
 107 frequency. The simplified formula is used to fit the AC iron loss data in this paper. According to the
 108 tested results of iron loss, the values of “ k_h ” and “ N ” can be fitted, as shown in Figure 3 (b) ~ (f).
 109 The different color formulas represent the fitting results of different frequencies. The prediction of
 110 iron loss through the formula - $P_t = k_t B_m^N$ is based on determining of “ k_h ” and “ N ”.

111 Figure 4 (a) and (b) depict the results of “ k_h ” and “ N ”. The different color formulas represent
 112 the “ k_h ” and “ N ” fitting results of different frequencies. Based on this fitting results, we can
 113 calculate the values of “ k_h ” and “ N ” at other frequencies. And then, “ k_h ” and “ N ” are taken into AC
 114 iron loss formula to predict the iron loss at other frequencies, such as 1.3 kHz, 4 kHz. From the
 115 Figure 4 (a) and (b) fitting results, “ k_h ” and “ N ” can be gained at 1.3 kHz, 4 kHz and core losses
 116 prediction results are shown in the Figure 4 (c) and (d). In order to verify the accuracy of the
 117 prediction, iron losses were tested and compared at 1.3 kHz and 4 kHz. From Figure 4 (c) and (d),
 118 the calculated value was found to be in a good agreement with the actual test results.
 119



120

121 **Figure 4.** (a) AC iron loss coefficient k_t and fit results; (b) AC iron loss factor N and fit results; The iron loss test
 122 result and calculation value at (c) 1.3 kHz frequency and (d) 4 kHz frequency.

123 In addition, the “AC Steinmetz law” ($P_t = k_{ac} B_m^n f^\alpha$) shows the total iron loss is affected by
 124 magnetic induction intensity and frequency. If this formula is used to predict the AC iron losses,
 125 first the exponent “ n ” value, “ α ” value and the coefficient “ k_{ac} ” should be fitted out from iron loss -
 126 magnetic induction intensity curves at a certain frequency or from iron loss - frequency curves at a
 127 certain magnetic induction intensity. However, at other frequency or magnetic induction intensity,
 128 the value of “ n ” and “ α ” will change. Here, we integrate the variable “ f ” into the coefficient “ k_t ”
 129 and determine the coefficient “ k_t ” and the exponent “ N ” of the formula - $P_t = k_t B_m^N$ by fitting.

130 Further to find out the dependence of “ k_t ” and “ N ” on the frequency by fitting. Thereby we can
131 predict the iron loss at other frequencies according to the formula - $P_t = k_t B_m^N$.

132 And when designing a core for using at a certain frequency or a certain frequency range, the
133 core loss and magnetic induction intensity are important indicators. Based on some iron losses data
134 and fitting results, designers can calculate the iron losses at different frequencies according to the
135 formula - $P_t = k_t B_m^N$. The design of magnetic induction intensity is not only related to the
136 composition and structure of the magnetic material, but also to the upper limit of the design of the
137 iron loss. According to the requirements of iron loss, designers can also calculate the design of
138 magnetic induction intensity.

139 4. Conclusions

140 Magnetic properties of the melt-spun Fe-6.5wt.%Si ribbons are investigated before and after
141 heat treatment at 1000 °C. DC properties are greatly improved, as well as the iron loss in the
142 frequency range of 400 Hz to 10 kHz. Above 10 kHz, the melt-spun ribbons exhibit lower total iron
143 loss compared with the annealed one.

144 A simplified formula based on Steinmetz law is proposed and verified to predict the AC iron
145 loss for high silicon steel ribbons in the range of 400 Hz to 5 kHz and the results are presented in this
146 paper According to iron losses data, “ k_t ” and “ N ” of the simplified formula - $P_t = k_t B_m^N$ can be
147 determined, and the AC iron losses can be predicted. The method developed in this work could be
148 used for other magnetic materials to predict AC iron loss with great ease.
149

150 **Acknowledgments:** Financial supports from the National Natural Science Foundation of China (No. U1660115,
151 51471031 and 51301019) are gratefully acknowledged.

152 **Author Contributions:** All co-authors have contributed substantially to the paper. Shuai Wang conceived,
153 designed and performed the experiments; Biao Chen contributed to the magnetic properties test; Shuai Wang
154 wrote the manuscript; Yongfeng Liang, Feng Ye and Junpin Lin supervised the work.

155

156 **Conflicts of Interest:** The authors declare no conflict of interest.
157

158 References

159

- 160 1. Bozorth, R.M. *Ferromagnetism*, Van Nostrand-Reinhold: New York, USA, 1951; 595, pp. 50-52,
161 0-7803-1032-2.
- 162 2. Viala, B.; Degauque, J.; Baricco, M.; Ferrara, E.; Pasquale, M.; Fiorillo, F. Magnetic and mechanical
163 properties of rapidly solidified Fe-Si 6.5 wt% alloys and their interpretation. *J. Magn. Magn. Mater.*
164 **1996**, *160*, 315-317, 10.1016/0304-8853(96)00209-0.
- 165 3. Haiji, H.; Okada, K.; Hiratani, T.; Abe, M.; Ninomiya M. Magnetic properties and workability of 6.5%
166 Si steel sheet. *J. Magn. Magn. Mater.* **1996**, *160*, 109-114, 10.1016/0304-8853(96)00128-X.
- 167 4. Li, H.; Liang, Y.F.; Ye, F. Effect of heat treatment on ordered structures and mechanical properties of
168 Fe-6.5 mass% Si Alloy. *Mater. Trans.* **2015**, *56*, 759-765, 10.2320/matertrans.M2014451.
- 169 5. Liu, S.Q.; Cui C.X.; Wang X.; Li N.; Shi J.J.; Cui S.; Chen P. Effect of Cooling Rate on Microstructure
170 and Grain Refining Behavior of In Situ CeB₆/Al Composite Inoculant in Aluminum. *Metals* **2017**, *7*, 204,
171 10.3390/met7060204.
- 172 6. Tan X.; Li H.Y.; Xu H.; Han K.; Li W.D.; Zhang F. A Cost-Effective Approach to Optimizing
173 Microstructure and Magnetic Properties in Ce₁₇Fe₇₈B₆ Alloys. *Materials* **2017**, *10*, 869,
174 10.3390/ma10080869.
- 175 7. Liang, Y.F.; Wang, S.; Li, H.; Jiang, Y.M.; Ye, F.; Lin, J.P. Fabrication of Fe-6.5 wt% Si ribbons by melt
176 spinning method on large scale. *Adv. Mater. Sci. Eng.* **2015**, *2015*, 296197, 10.1155/2015/296197.
- 177 8. Palmer, J.; Thompson, C.V.; Smith, H.I. Grain growth and grain size distributions in thin germanium
178 films. *J. Appl. Phys.* **1987**, *62*, 2492-2497, 10.1063/1.339460.

- 179 9. Steinmetz, C.P. On the law of hysteresis. *P. IEEE* **1984**, *72*, 197-221, 10.1109/PROC.1984.12842.
- 180 10. Kollár, P.; Olekšáková, D.; Vojtek, V.; Füzér, J.; Fáberová, M.; Bureš, R. Steinmetz law for ac
- 181 magnetized iron-phenolformaldehyde resin soft magnetic composites. *J. Magn. Magn. Mater.* **2017**,
- 182 *424*, 245-250, 10.1016/j.jmmm.2016.10.060.
- 183 11. Svensson, L.; Frøgner, K.; Jeppsson, P.; Cedell, T.; Andersson, M. Soft magnetic moldable composites:
- 184 Properties and applications. *J. Magn. Magn. Mater.* **2012**, *324*, 2717-2722, 10.1016/j.jmmm.2012.03.049.